Detection of nanoscale structural changes in bone using random lasers

Qinghai Song,[1] Zhengbin Xu,[1] Seung Ho Choi,[1] Xuanhao Sun,[1] Shumin Xiao,[2] Ozan Akkus[1], and Young L. Kim[1,*]

[1]*Weldon School of Biomedical Engineering, Purdue University, West Lafayette, IN 47907*
[2]*School of Electrical and Computer Engineering and Birck Nanotechnology Center, Purdue University, West Lafayette, IN 47907*
**youngkim@purdue.edu*

Abstract: We demonstrate that the unique characteristics of random lasing in bone can be used to assess nanoscale structural alterations as a mechanical or structural biosensor, given that bone is a partially disordered biological nanostructure. In this proof-of-concept study, we conduct photoluminescence experiments on cortical bone specimens that are loaded in tension under mechanical testing. The ultra-high sensitivity, the large detection area, and the simple detection scheme of random lasers allow us to detect prefailure damage in bone at very small strains before any microscale damage occurs. Random laser-based biosensors could potentially open a new possibility for highly sensitive detection of nanoscale structural and mechanical alterations prior to overt microscale changes in hard tissue and biomaterials.

OCIS codes: (280.1415) Biological sensing and sensors; (140.4780) Optical resonators; (140.2050) Dye lasers; (170.3660) Light propagation in tissues.

References and links

1. H. Cao, "Review on latest developments in random lasers with coherent feedback," J.Phys. A Math. Gen. **38**(49), 10497–10535 (2005).
2. D. S. Wiersma, "The physics and applications of random lasers," Nat. Phys. **4**(5), 359–367 (2008).
3. P. Pradhan, and N. Kumar, "Localization of light in coherently amplifying random media," Phys. Rev. B Condens. Matter **50**(13), 9644–9647 (1994).
4. H. Cao, Y. G. Zhao, S. T. Ho, E. W. Seelig, Q. H. Wang, and R. P. H. Chang, "Random laser action in semiconductor powder," Phys. Rev. Lett. **82**(11), 2278–2281 (1999).
5. R. C. Polson, A. Chipouline, and Z. V. Vardeny, "Random lasing in pi-conjugated films and infiltrated opals," Adv. Mater. **13**(10), 760–764 (2001).
6. R. C. Polson, and Z. V. Vardeny, "Random lasing in human tissues," Appl. Phys. Lett. **85**(7), 1289–1291 (2004).
7. A. Tulek, R. C. Polson, and Z. V. Vardeny, "Naturally occurring resonators in random lasing of pi-conjugated polymer films," Nat. Phys. **6**(4), 303–310 (2010).
8. X. Wu, W. Fang, A. Yamilov, A. A. Chabanov, A. A. Asatryan, L. C. Botten, and H. Cao, "Random lasing in weakly scattering systems," Phys. Rev. A **74**(5), 053812 (2006).
9. C. Vanneste, P. Sebbah, and H. Cao, "Lasing with resonant feedback in weakly scattering random systems," Phys. Rev. Lett. **98**(14), 143902 (2007).
10. S. Mujumdar, M. Ricci, R. Torre, and D. S. Wiersma, "Amplified extended modes in random lasers," Phys. Rev. Lett. **93**(5), 053903 (2004).
11. S. Mujumdar, V. Turck, R. Torre, and D. S. Wiersma, "Chaotic behavior of a random laser with static disorder," Phys. Rev. A **76**(3), 033807 (2007).
12. R. C. Polson, and Z. V. Vardeny, "Organic random lasers in the weak-scattering regime," Phys. Rev. B **71**(4), 045205 (2005).
13. Q. Song, S. Xiao, Z. Xu, J. Liu, X. Sun, V. Drachev, V. M. Shalaev, O. Akkus, and Y. L. Kim, "Random lasing in bone tissue," Opt. Lett. **35**(9), 1425–1427 (2010).
14. R. O. Ritchie, M. J. Buehler, and P. Hansma, "Plasticity and toughness in bone," Phys. Today **62**(6), 41–47 (2009).
15. Q. Song, S. Xiao, Z. Xu, V. M. Shalaev, and Y. L. Kim, "Random laser spectroscopy for nanoscale perturbation sensing," Opt. Lett. **35**(15), 2624–2626 (2010).
16. X. H. Sun, J. Hoon Jeon, J. Blendell, and O. Akkus, "Visualization of a phantom post-yield deformation process in cortical bone," J. Biomech. **43**(10), 1989–1996 (2010).
17. H. S. Gupta, W. Wagermaier, G. A. Zickler, D. Raz-Ben Aroush, S. S. Funari, P. Roschger, H. D. Wagner, and P. Fratzl, "Nanoscale deformation mechanisms in bone," Nano Lett. **5**(10), 2108–2111 (2005).

#136122 - $15.00 USD Received 5 Oct 2010; revised 9 Nov 2010; accepted 9 Nov 2010; published 11 Nov 2010

18. O. Akkus, "Elastic deformation of mineralized collagen fibrils: an equivalent inclusion based composite model," J. Biomech. Eng. **127**(3), 383–390 (2005).
19. K. L. van der Molen, R. W. Tjerkstra, A. P. Mosk, and A. Lagendijk, "Spatial extent of random laser modes," Phys. Rev. Lett. **98**(14), 143901 (2007).
20. H. E. Türeci, L. Ge, S. Rotter, and A. D. Stone, "Strong interactions in multimode random lasers," Science **320**(5876), 643–646 (2008).

1. Introduction

Random lasers are multiple-scattering-induced lasers that do not rely on any well-configured resonant cavities, because in random lasers, resonant cavities are randomly self-formed due to multiple scattering [1,2]. After light localization for random lasing was theoretically predicted [3], several experimental studies were conducted to understand the origin of multiple discrete peaks in random lasing emission (specifically coherent random lasers) in many types of material systems ranging from strongly scattering regimes to weakly scattering regimes [4–9]. Currently, the exact origin of coherent random lasers is understood on the basis of two mechanisms [7]: i) Spontaneous emission events can be significantly amplified through a long light path, showing chaotic behavior (i.e. amplified spontaneous emission) [10,11]. ii) Deterministic laser cavities can be randomly formed due to multiple scattering in disorder gain media and thus the narrow emission peaks correspond to physical laser cavity modes (i.e. coherent random lasers) [6,7,12]. In particular, most of the previous studies strongly imply that resonant modes in coherent random lasers should be closely correlated with the structural properties of the random media such as refractive index and internal structure variations.

Although random lasers have been the objective of intensive investigations, they still await novel applications. In our previous study [13], we reported that bone tissue can be an ideal material for random lasers, because bone is a biological nanostructured dielectric in an intermediate regime between ordered photonic structures and completely disordered nanostructures [14]. In our recent study [15], we further demonstrated potential advantages of the random laser spectroscopic technique including ultra-high sensitivity to nanoscale perturbations, large detection areas/volumes, and easy detection. Because the properties of bone at the microscale have been intensively studied for better understanding how bone deforms and fractures in terms of plasticity and toughness, one intriguing application of random lasers is to study the mechanical and structural properties of bone. As the first step toward this research direction, in this study we demonstrate, for the first time to our knowledge, that random lasing in bone can be used to assess prefailure nanoscale deformation in bone at small strains before any conventional damage occurs. Specifically, we report that the random laser-based spectroscopic method can allow the detection of nanoscale structural perturbations in bone under mechanical testing, and that our simple numerical study can provide insight on possible underlying mechanisms at bone prefailure stages.

2. Materials and methods

2.1. Bone specimen preparations

We prepared for cortical bone specimens from bovine femurs following the previous preparation procedure [16]. In brief, we sectioned longitudinal block beams from the diaphysis of bovine femurs using a precision saw. We used a mill to make a v-shaped notch, which can serve to concentrate the stress at the root of the notch. We further sectioned the notched block into thin wafers and polished them by using polishing papers with progressively finer grade and finally with 0.3-μm alumina powder. The dimension of the final cortical bone specimen was approximately 50 mm x 4 mm x 200 μm. Figure 1(a) illustrates that the longest dimension of the specimen was along the longitudinal orientation of the bone structure (i.e. the mineralized collagen fibrils are relatively aligned in this orientation). To assess physical parameters of bone structure for numerical studies, we obtained scanning electron microscopy (SEM) images. As shown in Fig. 1(b), the magnification SEM image of our cortical bone specimen displays the profiles of the relatively well-aligned collagen fibers

#136122 - $15.00 USD Received 5 Oct 2010; revised 9 Nov 2010; accepted 9 Nov 2010; published 11 Nov 2010

embedded in the matrix. For photoluminescence experiments, we immersed the specimens in a common laser dye solution (i.e. Rhodamine 800 in ethanol with a weight ratio of 0.3%).

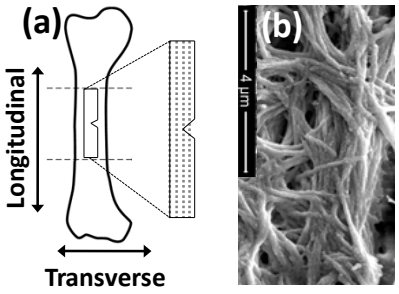

Fig. 1. (a) Schematic illustration of bone specimen preparation. (b) Representative SEM image of the bone specimen. The collagen fibrils with the diameter of ~100 nm are relatively well-aligned.

2.2. Photoluminescence experiments

In optical lasing measurements, to optically pump the specimen, we used a tunable pulsed laser (optical parametric amplifier pumped with a Ti:sapphire regenerative amplifier). The pump laser wavelength was at ~690 nm, which is the absorption peak of Rhodamine 800. The pulse width was 100 fs and the repetition rate was 1 KHz. The pumping beam was focused normally onto the specimen through a cylindrical lens to form a narrow strip of ~150 μm × 5 mm along the notch direction as shown in Fig. 2. The pumping strip was along the transverse orientation of the bone structure to maximize light confinement for random lasing. When the pumping strip was along the longitudinal orientation, random lasing action was hardly observed at the sample pumping power, supporting the idea that the partially disordered bone structure in the transverse orientation is primarily responsible for light confinement. The emission light was collected with an acquisition time of 1 second from the side using a fiber bundle through a lens and coupled to a spectrometer with the resolution of ~0.2 nm. The pumping illumination was blocked by a 20-nm bandpass filter centered at 720 nm. The specimen was covered with a microscope slide. Kimwipes were connected to an ethanol reservoir below the specimen to keep the specimen wet and to avoid the aggregation of the laser dye.

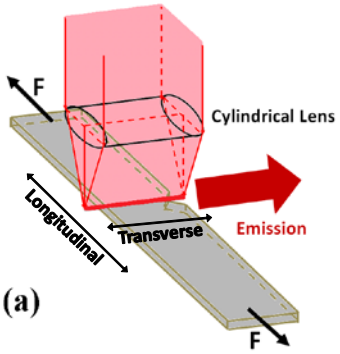

Fig. 2. Photoluminescence experiment setup. A narrow strip of the Ti:sapphire laser illumination is normally focused onto the surface of bone tissue along the transverse orientation.

#136122 - $15.00 USD Received 5 Oct 2010; revised 9 Nov 2010; accepted 9 Nov 2010; published 11 Nov 2010

2.3. Mechanical testing

We used a miniaturized tensile testing device to introduce tensile force to the bone specimen. Using this device, we can apply tensile force onto the specimen symmetrically, which eliminates the shift of the notch tip during loading. We acquired sequential data for each specimen before loading, under peak loading, and after removal of the loading. To induce minimal yet detectable deformation at the stress concentrator (i.e. the notch area), the tensile force applied on the specimen was 2.0 lbs (= 8.9 N). We also performed digital image correlation (DIC) analysis on the bone specimen immersed in the ethanol solution to estimate strain under the peak loading [16]. Under the current experimental conditions, the DIC analysis showed that a peak strain can be as high as −0.2% (i.e. compression) at around the notch area along the transverse orientation. In the previous study [16], opacity in transmission microscopic images was formed when an absolute value of strain was ~1.0% in the cortical bovine bone specimen that was loaded in tension with the tensile load of ~20–40 N. Under our experimental conditions, we confirmed that no opacity zones, microcracks, or other damage occurred by examining the specimen using a microscope in both reflectance and transmission modes.

2.4. Numerical simulation

To gain a better understanding of our experimental results, we conducted a numerical study using a finite element method of electromagnetic analysis, similarly to our previous studies [13,15]. We intended to address possible underlying nanoscale deformation mechanisms that can be attributable to the random laser emission spectra. As illustrated in Fig. 3, we approximated the bone structure to a quasi-one-dimensional (1D) multilayer structure consisting of the collagen fibrils and the interfibrillar space. This is because the narrow strip of the pumping illumination was along the transverse orientation of the cortical bone (i.e. perpendicular to the orientation of the mineralized collagen fibrils). We simulated passive modes without gain or absorption (i.e. the refractive indices in the system are real numbers) using Comsol Multiphysics 3.5a. In this case, the wavevector is a complex number: $\kappa = \mathrm{Re}(\kappa) + i*\mathrm{Im}(\kappa)$, which contains both resonant frequencies and losses. We obtained the eigenvalues of the system to estimate resonant modes and quality (Q) factors ($= |\mathrm{Re}(\kappa)/(2*\mathrm{Im}(\kappa))|$). In our simulation, only TE polarization was modeled. 300 mineralized collagen fibril layers (thickness = d_f) are separated by the interfibrillar layer (thickness = d_s). To mimic the partially disordered structure, we randomly varied each fibril thickness d_f from 50 to 125 nm, the distance between each fibril d_s from 25 to 100 nm, and the angle of each fibril θ_f from −0.5 to 0.5°, respectively. The refractive indexes of collagen fibril layer and separation matrix layer between each fibril were set to be 1.6 and 1.4, respectively. The mineralized collagen fibrils can be subject to elongation [17] and the mineral content within the collagen fibrils can lower the Poisson's ratio [18]. Thus, a subtle thickness reduction in the mineralized collagen fibrils would be primarily attributable to the structural variation in our experiment. To model this potential structural change that can be derived from the tensile load in the longitudinal orientation, we reduced the thickness of each mineralized collagen fibril layer by 0.2%.

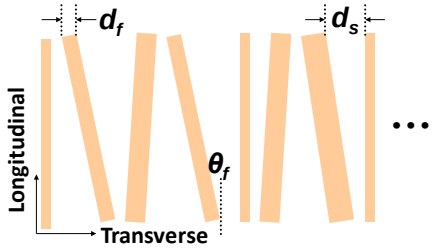

Fig. 3. Schematic of the quasi-1D multilayer structure. Each brown bar represents each collagen layer. Our numerical sample consists of 300 layers with a small titled angle to mimic the partially disordered bone structure under our experimental conditions.

#136122 - $15.00 USD Received 5 Oct 2010; revised 9 Nov 2010; accepted 9 Nov 2010; published 11 Nov 2010

3. Results

3.1. Confirmation of coherent random lasing action

We first confirmed coherent random lasing action from the bone specimen infiltrated with the laser dye before applying any loading. Figure 4(a) shows a typical random laser emission spectrum at the pumping power of 80 mW. The discrete and randomly distributed peaks in the emission spectrum are clearly observed, although the detailed spectral features are masked by the spectral resolution of the spectrometer (~0.2 nm). In Fig. 4(b), we plot the emission intensity as a function of the pumping power. A clear laser threshold behavior at ~45 mW confirmed the lasing action in the bone specimen.

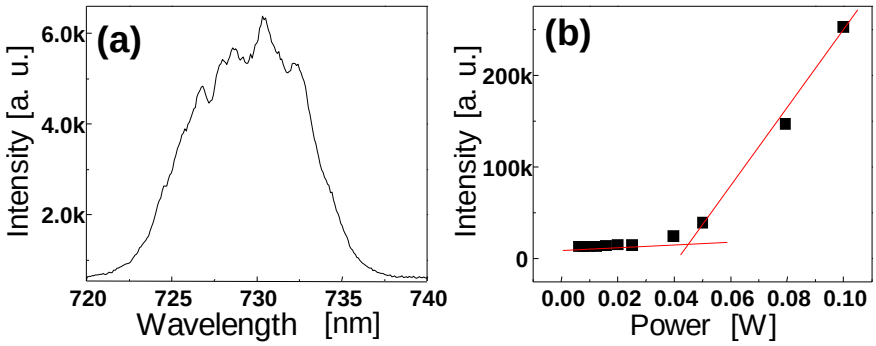

Fig. 4. (a) Representative emission spectrum measured from the side of the bone specimen infiltrated with Rhodamine 800 before loading. The pump intensity was kept at 80 mW. (b) The output emission intensity as a function of pumping power. A clear laser threshold can be seen at ~45 mW.

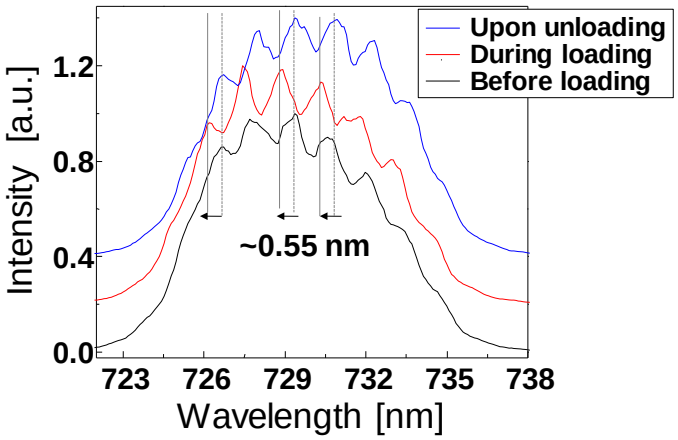

Fig. 5. Lasing emission spectra recorded before loading (black solid line), under peak loading (red solid line), and after removal of loading (blue solid line). A clear shift of ~0.55 nm in all of the emission peaks can be observed under the peak loading (i.e. 2.0 lbs). After removal of the loading, the laser peaks restored to the original peak positions. The vertical gray lines are plotted to clearly visualize the wavelength shift. The spectra are shifted vertically for the clear visualization of each emission spectrum in the vertical axis.

3.2. Spectral changes in random lasing emission during peak loading

We further examined emission spectral changes at the notch area before loading, under peak loading, and after removal of the loading, while keeping the same experiment conditions and the same pumping power at 80 mW. In Fig. 5, representative spectra are normalized and vertically shifted for the clear visualization of each emission spectrum. Before the loading, the

#136122 - $15.00 USD Received 5 Oct 2010; revised 9 Nov 2010; accepted 9 Nov 2010; published 11 Nov 2010

discrete laser peaks (the black curve in Fig. 5) can be observed. Under the peak loading (i.e. 2.0 lbs), the random laser emission peaks (the red curve) is clearly shifted to the left by ~0.55 nm. After removal of the loading, most of them (the blue curve) return to the original spectrum. This experimental result strongly indicates that a structural alteration (i.e. compression along the transverse orientation) occurred in the pumping area during the peaking loading and this alteration disappeared after removal of the loading.

3.3. Lasing emission spectral changes induced from nanoscale structural alterations

We numerically studied that the possible structural alteration under our experimental conditions can induce spectral changes in the random lasing emission. The primarily responsible structural alteration in our experiments would be the thinning of the mineralized collagen fibrils. In this numerical study, the thickness of each collagen fibril layer was reduced by 0.2% of the original value of each collagen layer. Figure 6(a) shows the representative eigenvalues before and after the thinning of the collagen fibril layer. We arbitrarily selected one of the high Q eigenvalues and visualized the electric field. Figure 6(b1) and (b2) show the electric fields before and after the structural change, respectively. In this case, the eigenvalue changed from $\kappa = 8.992 - 1.060*10^{-2}*i$ [1/μm] (the blue solid dot) to $\kappa = 8.993 - 1.060*10^{-2}*i$ [1/μm] (the red solid dot), resulting in a spectral shift of ~0.08 nm. While the spatial distributions of both the electric fields are relatively preserved covering the large area, the overall intensity increases after the thinning of the collagen fibril layers. Although other internal structural changes may contribute to the spectral change in the random laser emission, this simulation result supports the idea that the spectral properties of the random laser emission can be highly sensitive to nanoscale structural alterations.

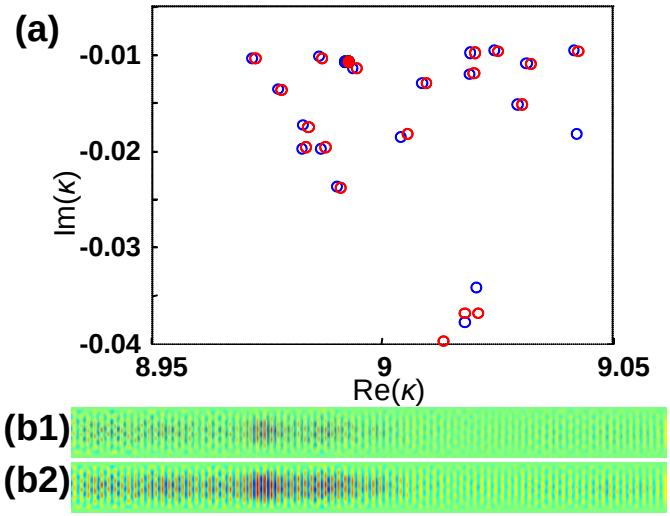

Fig. 6. (a) Representative eigenvalues of the system. The blue circles are the eigenvalues of the original structure, while the red circles are the eigenvalues after reducing the thickness of each collagen fibril layers by 0.2%. (b1) Electric field intensity distribution at $\kappa = 8.992 - 1.060*10^{-2}*i$ [1/μm] (the blue solid dot in (a)) (b2) Electric field intensity distribution at $\kappa = 8.993 - 1.060*10^{-2}*i$ [1/μm] (the red solid dot in (a)).

4. Discussion

4.1. Possible origins of the random laser spectral alteration

A displacement of the while specimen might induce the spectral change in the random laser emission during the loading. However, this was highly unlikely to occur under our experimental conditions, because the loading stage maintained the observation region fixed during the loading. In addition, as shown in Fig. 5, the emission spectra contain the periodic

#136122 - $15.00 USD Received 5 Oct 2010; revised 9 Nov 2010; accepted 9 Nov 2010; published 11 Nov 2010

patterns over the wavelength, possibly due to the boundary effect of the thin specimen. However, the emission spectrum under the peak loading possessed the same number of the laser emission peaks and the similar spacing among the laser emission peaks, while the overall spectral shape was slightly shifted to the shorter wavelength. This means that most of the lasing modes remained within the pumping area, given that lasing modes are formed only if the field distribution overlaps with the gain region [19,20]. Collectively, our results strongly support that the idea that the spectral shift in the lasing emission under the peak loading was caused by subtle structural alterations at the extremely small strain.

4.2. Drawbacks of our current study

The dehydration of the bone specimen may have changed the mechanical properties of the cortical bone specimen in our photoluminescence experiments, because the solvent of Rhodamine 800 was ethanol. However, we intended to demonstrate the sensitivity of coherent random lasing to nanoscale structural alterations as a proof-of-concept study. Thus, this issue would not be critical in our current study. In our numerical study, the thinning of the collagen fibrils may account for one of several possible nanoscale deformation mechanisms that can occur in our experimental conditions. For example, shear deformation of the interfibrillar matrix [17] or debonding of mineral crystals from the neighboring collagen fibrils [16] can induce spectral changes in the random laser emission. Another drawback of our current study is the lack of quantitative comparison with other convention techniques at such a small strain level for bone (e.g. electron microscopy, atomic force microscopy, or x-ray diffraction). In other words, the exact structural origin in the nanoscale deformation during this level of peak loading has not been determined by a conventional nanoscale measurement. We note that x-ray diffraction methods are typically used to study relatively higher strains compared with our study. With fairly simple sample preparation, our random laser-based method allows the detection of extremely small strains and deformation.

5. Conclusion

We demonstrated that random lasers can be used as a mechanical or structural sensor to detect nanoscale deformation and prefailure damage in bone, and that the simple numerical study supports such feasibility. Although conventional nanoscale measurements such as electron microscopy, x-ray diffraction, and atomic force microscopy are highly valuable tools to study nanoscale mechanical and structural characteristics of hard tissue and biomaterials, they have limitations and restrictions in specific experimental situations. In this respect, our results from this pilot study suggest that random laser-based methods could potentially find their own unique applications.

Acknowledgments

This project was supported in part by grants from Purdue Research Foundation and NIH 1R03CA153982. We thank Umut Atakan Gurkan for the SEM image of the bone specimen.

#136122 - $15.00 USD Received 5 Oct 2010; revised 9 Nov 2010; accepted 9 Nov 2010; published 11 Nov 2010